

# PHYSICAL REVIEW B

## CONDENSED MATTER

THIRD SERIES, VOLUME 39, NUMBER 18

15 JUNE 1989-II

### Symmetry breaking in nitrogen-doped amorphous carbon: Infrared observation of the Raman-active *G* and *D* bands

J. H. Kaufman and S. Metin

IBM Research Division, Almaden Research Center (K33/802), 650 Harry Road, San Jose, California 95120-6099

D. D. Saperstein

IBM Corporation (E35/13), 5600 Cottle Road, San Jose, California 95193

(Received 7 October 1988; revised manuscript received 8 February 1989)

We report the preparation of hard nitrogenated amorphous carbon films doped with as much as 20 at. % nitrogen. The nitrogen groups created by doping do not dramatically affect the film structure, but are found to break symmetry in  $sp^2$  domains causing the Raman-active *G* ("graphitic") and *D* ("disordered") bands to become ir active. Elemental analysis of the films together with the infrared spectra shows that about one in six of the carbons are replaced by nitrogen. Also observed in the infrared spectrum are nitrile (and possibly isonitrile) groups which demonstrate for the first time the existence of *sp* carbon in amorphous carbon films.

#### INTRODUCTION

Amorphous carbon films are extremely useful for protecting thin-film disks and other surfaces.<sup>1-3</sup> These films can be made under a variety of conditions including argon-ion sputtering of a carbon target<sup>4</sup> and plasma deposition of hydrocarbon gas.<sup>5,6</sup> Hydrogenated amorphous carbon (*a*-C:H) can be quite hard, approaching the hardness of diamond (so-called diamondlike carbon or "*i*-carbon"),<sup>7,8</sup> and the surface can be sufficiently uniform to provide an effective barrier against corrosion. *i*-carbon films are typically insulating, which may be advantageous in some applications.<sup>7,8</sup> On a microscopic scale, the term amorphous carbon is not well defined. Amorphous hard carbons do not exhibit a diamond structure when measured either by x-ray diffraction or Raman spectroscopy.<sup>9</sup> Instead they have regions of  $sp^2$  microdomains which are of the order of 5–20 Å in diameter. These "graphitic" microdomains are characterized by a diffuse x-ray powder pattern and by the appearance of a broad Raman band at 1575  $cm^{-1}$  (the *G* band arising from the symmetric  $E_{2g}$  mode) and an overlapping broad band at 1360  $cm^{-1}$  which is a measure of the disorder of the carbon (*D* band arising from an  $A_{1g}$  mode whose intensity is quite sensitive to the size of the microdomains).<sup>10-13</sup> Recently, the scanning tunneling microscope (STM) has imaged ordered domains directly with atomic resolution.<sup>14</sup> In addition to the  $sp^2$  carbon in the microdomains there may be  $sp^3$  carbon, as well as other functionalities not easily observed. Often, trace impurities are also observed by elec-

tron spectroscopy for chemical analysis (ESCA) and other techniques.<sup>3</sup>

Recently, there have been reports of the use of nitrogen for doping amorphous carbon films.<sup>15,16</sup> Several motivations exist for investigating nitrogenated carbons. One can imagine that nitrogenated carbon may form a phase similar to amorphous silicon nitride<sup>15,17</sup> which could be even harder than undoped amorphous carbon. Nitrogen may increase the basicity of the films making the surface more hospitable for the retention of acid groups. Nitrogenated carbons are likely to exist in outer space,<sup>15,18</sup> and it is convenient to study the infrared properties of these materials in an Earth-based laboratory so as to facilitate our understanding of the interstellar dust. The infrared spectra of amorphous carbons are typically featureless (sometimes not even exhibiting CH vibrations).<sup>19</sup> However, infrared spectroscopy of nitrogenated carbon made by previous workers reveals the existence of numerous bands including C=N (imine), C≡N (nitrile), NH<sub>2</sub> (amine), and CH<sub>2</sub> (methylene) groups.<sup>15</sup> The observation of these modes has been used as evidence that nitrogenated carbon is more like polymeric *a*-C:H than *i*-carbon.<sup>15</sup>

We report the fabrication of a new class of nitrogenated carbons which retain the basic structure and properties of the undoped hard carbon. Our investigations demonstrate that although the nitrogen appears to alter the amount of  $sp^2$  carbon observed in the infrared spectrum, Raman spectroscopy indicates that the actual structure of the  $sp^2$  microdomains is unaffected by the nitrogen. These facts may be reconciled by noting that the

*G* band, which is usually ir forbidden in the two-dimensional sheet, becomes ir active when N is substituted in the graphitic microdomains.  $^{15}\text{N}$  isotopic labeling supports this assertion. In addition to its striking effect on the *G* band, nitrogen is also found to combine with carbon to produce two species of *sp* carbon. When hydrogen is also present, the polymeric hydrocarbon ( $sp^3$ ) content is reduced as the hydrogen is captured in amino groups.

### EXPERIMENT

Carbon films were deposited on 1-in.-diam (100)-oriented *p*-type doped silicon substrates (0.1  $\Omega$  cm). Each substrate was cleaned by immersion in concentrated sulfuric acid followed by rinsing in deionized water for 5 min. The substrates were dried in a hot isopropyl alcohol oven for 2 min. For the purpose of grazing-angle ir measurements, some of the substrates were coated with 3000  $\text{\AA}$  of aluminum (over a 50- $\text{\AA}$  chromium adhesion layer). Deposition was accomplished in a (Balzers) turbo-pumped stainless-steel high-vacuum system (Vacuum Generators, Kurt Lesker Co.) The base pressure of the system was  $5 \times 10^{-8}$  Torr. The feed gas contained 1 mTorr of cyclopentane (vapor pressure was 320 Torr at 298 K) plus 7 mTorr of carrier gas. The particular hydrocarbon used is apparently unimportant; similar material has been produced using cyclohexane and methane. The carrier gas was composed of a  $\text{N}_2$ -Ar mixture in a variable ratio from 0% to 95%. Pressure was measured by a Vacuum General capacitance manometer. Gas flow was controlled by two Vacuum General Dynamass FM-4 regulators. The mass-flow ratio was fixed to provide the desired nitrogen-argon ratio [the total gas flow was approximately 25 sccm ( $\text{cm}^3/\text{min}$  at STP)]. Total pressure was held fixed at 8 mTorr throughout the deposition. At these flow rates the maximum relative nitrogen concentration  $[\text{N}]/([\text{N}] + [\text{C}])$  is approximately 58 at.%. The plasma was maintained by a rf magnetron sputter source operating at 500 W (Eratron), using a graphite target. The substrates were held in an electrically isolated, water-cooled, rotating carousel. They were biased to  $-350$  V dc with a Sloan 7/7 High Voltage Supply. The dc bias was set to provide positive-ion bombardment of the substrates. When no bias is used (or when insulating substrates are used) the resulting films are soft and polymeric. With bias, the undoped films were harder than 15 GPa (determined by a diamond microindenter). Sputter deposition alone proceeds at a rate of about 100  $\text{\AA}/\text{h}$  whereas plasma deposition with the hydrocarbon proceeds at over 2000  $\text{\AA}/\text{h}$ . Therefore, virtually all of the carbon deposited comes from the hydrocarbon feed gas (and *not* from the graphite target). All measurements described here were made on films deposited for 60 min. Film thickness was measured by ellipsometry, and scanning electron microscopy (SEM) of the cross section. All films are about 2000  $\text{\AA}$  thick (see below).

### CHARACTERIZATION

To obtain the nitrogen content of our films, elemental analysis of the samples was accomplished by x-ray photo-

electron spectroscopy (XPS), electron microprobe analysis (EMPA), Rutherford backscattering (RBS), and x-ray fluorescence (XRF). The XRF data were calibrated by the RBS data for the most heavily nitrogenated carbon. Film structure was studied by scanning electron microscopy and x-ray diffraction. Optical properties were measured by NIR-VIS-UV photothermal deflection, Raman and infrared spectroscopy.

**XPS (ESCA).** A Surface Science Instruments (SSI) model 501 ESCA system (x rays in, electrons out) was used for the measurements. Both surface studies and depth profiling were performed. In addition to carbon and nitrogen, the spectra showed trace amounts of fluorine (only on the surface) which probably came from traces of pump oil in the ESCA chamber itself. Depth profiling demonstrated that the relative nitrogen concentration was constant through the bulk of the different samples. Trapped argon was also observed by this technique. No oxygen was observed in the bulk, though traces were found on the surface (the samples were exposed to ambient for about one month before the ESCA measurements).

**Electron microprobe analysis.** A Cameca 5X50 Electron Microprobe (electrons in, x rays out) was used to study the composition of the films. The nitrogen *K $\alpha$*  and carbon *K $\alpha$*  lines were measured and averaged over well-separated areas on the sample.

**RBS.** Rutherford backscattering was measured using a National Electrostatic Corp. spectrometer. The incident energy of the He-ion beam was 2.257 MeV. A total charge of 50  $\mu\text{C}$  was collected for each sample. The detection angle was  $160^\circ$ , and the helium beam was aligned along a silicon lattice channel (of the substrate) to reduce the Si signal. The RBS also indicated that the relative nitrogen concentration was constant through the film.

**XRF.** X-ray fluorescence (x rays in, x rays out) was performed with a Rigaku model No. 3070. These measurements had to be calibrated for our carbons. Calibration was accomplished using the RBS measurement of the most heavily doped sample. RBS was the most accurate technique employed.

**PDS.** Photothermal deflection spectroscopy uses the optical heating of a film to measure absorbance. When a modulated light beam is incident on a thin carbon film, the absorbed energy is converted to a periodic heat pulse radiating from the surface. A second probe beam is focused and aligned along the surface at the point of heating. The probe beam will experience a deflection due to the change in index of refraction of the surrounding medium (in this case liquid "Fluorinert"). The deflection can then be detected at a distance and converted into a measure of the absorbance (the greater the absorbance the larger the deflection).

The heating beam was the monochromatized output of a chopped xenon arc lamp. A 1-mW He-Ne laser was used for the probe beam, and its deflection was measured by a standard quadrant position sensor.

**Raman.** Raman spectra were obtained using an argon-ion laser, a triple monochromator (Spex Industries), and a water-cooled RCA C31034 photomultiplier.

Resolution was  $2\text{ cm}^{-1}$  degraded to  $4\text{ cm}^{-1}$  after a three-point smoothing of the data. Excitation wavelengths of 488 and 514.5 nm were used. Angle of incidence of the laser was  $60^\circ$  measured with respect to the surface normal. The angle of collection was  $45^\circ$  normal to the surface with the optical axis of the spectrometer at a  $90^\circ$  angle with respect to the incident laser excitation. With this configuration the reflected laser beam just missed the edge of the collection lens. The Raman spectrum of the undoped sample exhibits a strong fluorescence background which is quenched by even low levels of nitrogen doping.

*ir.* Infrared spectra were recorded on an IBM Instruments IR/32 Fourier transform infrared spectrometer (FTIR) at  $2\text{ cm}^{-1}$  resolution using an ambient-temperature deuterated triglycine sulfate (DTGS) detector. The sample was held at an  $81^\circ$  angle ( $9^\circ$  off grazing) to enhance the reflection-absorption measurement of the infrared modes which have net dipole moments perpendicular to the plane of the film.<sup>20</sup> Approximately 20 000 scans were coadded to achieve the signal-to-noise ratio shown. Spectra were ratioed to a previously collected spectrum of an aluminum mirror. Slight differences between the reflectivity of the aluminum mirror and carbon-coated aluminum samples resulted from increased oxide and adventitiously deposited ambient organics.

## RESULTS AND DISCUSSION

The relative film composition  $[N]/[C]$ , excluding hydrogen, was determined by various techniques as a function of  $N_2$  partial pressure in the plasma. The results are summarized in Table I. The data, atomic percent nitrogen normalized to the C content, demonstrate that the relative nitrogen concentration in the film increases with the  $N_2$  partial pressure in the plasma, and saturates at 20 at. %. At this nitrogen content, the mechanical properties of the films do not change significantly. Other deposition parameters such as film thickness, plasma

composition, pressure, and bias were rigorously controlled to facilitate comparison of the doped and undoped films.

A good measure of the morphology of amorphous carbons is provided by Raman spectroscopy.<sup>1-3,9-13</sup> The Raman-active modes of all amorphous carbon samples are found at approximately  $1575\text{ cm}^{-1}$  (*G* band, *G* means "graphitic") and  $1360\text{ cm}^{-1}$  (*D* band, *D* means "disordered"). The *D* band should not be confused with the sharp Raman line of diamond observed at  $1332\text{ cm}^{-1}$ . The *G* band arises from a symmetric vibration also observed in graphite.<sup>21,22</sup> This vibration is shown schematically in Fig. 1. Atoms *a* and *b* in the ring move with an opposing oscillation. Pairs in adjacent sheets (*a'* and *b'*) oscillate  $180^\circ$  out of phase with respect to *a* and *b*. For a single sheet (graphene), this vibration has  $E_{2g}$  symmetry and is ir forbidden because there is no change in dipole moment in the plane of the sheet. For graphite, which has a three-dimensional structure, this mode splits into the  $E_{2g}$  and  $E_{1u}$  modes.<sup>21</sup> The  $E_{2g}$  is the symmetric Raman-active *G* band ( $1584\text{ cm}^{-1}$ ), and the  $E_{1u}$  is weakly ir active ( $1588\text{ cm}^{-1}$ ) because the net dipole moment is small. In disordered  $sp^2$  carbons, the Raman *G* band broadens and shifts to lower wave numbers.<sup>9,12</sup> If there is no correlation between layers, the  $E_{1u}$  vibration is absent in the infrared spectrum because there is no perpendicular component to break the symmetry of the vibration. However, the Raman *D* band appears due to this disorder and is a manifestation of in-plane vibrational modes at the surface of the  $sp^2$  domains.<sup>9,10,12</sup> As the domain size increases, the intensity of the *D* band decreases with respect to the *G* band. The relative Raman intensity of the *D* and *G* bands is, therefore, a measure of the degree of order in an amorphous carbon sample. Recent work has shown that the Raman measurement is partly resonance enhanced.<sup>23</sup> The degree of enhancement may be required to extract precise domain-size information from the shape of the *G* and *D* bands.

In Fig. 2 the Raman spectra of the undoped and most heavily nitrogen-doped carbon samples are shown. The

TABLE I. Relative composition of film (excluding hydrogen).

at. % $N_2$ in plasma	[C] $\equiv$ 100				Estimated nitrogen fraction <sup>a</sup>
	EMPA	XRF	XPS	RBS	
0%	[N] < 1		[N] = 2.1		0
5%	[N] = 1.6 [Ar] = 1	[N] = 0	[N] = 5.3 [Ar] = 1.6	[N] = 2	2
25%	[N] = 10 [Ar] = 0.7	[N] = 3.1	[N] = 15		9
50%	[N] = 13.6 [Ar] = 0.5	[N] = 12.4	[N] = 16		15
75%		[N] = 19.1			18
90%		Calibration to RBS		[N] = 20.5 [Ar] = 0.06 [W] = 0.002	19
95%	[N] = 20 [Ar] = 0.1	[N] = 16	[N] = 20		20

<sup>a</sup>Calculated from fit to all data (see Fig. 6).

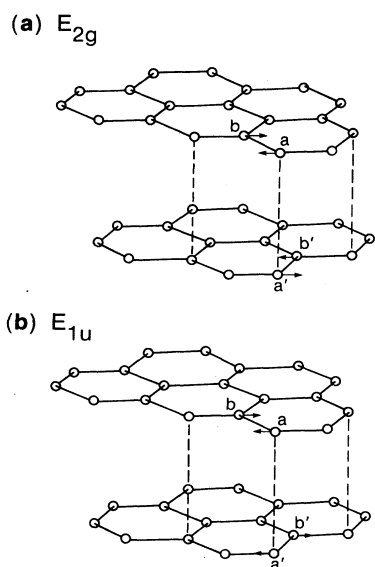


FIG. 1. The  $E_{2g}$  (a) and  $E_{1u}$  (b) modes in graphite (see text).

most striking feature in this data is the fact that the intensity ratio of the Raman  $G$  and  $D$  bands remains the same as the relative nitrogen content increases from 0 to 20 at. %. The  $G$  band is found to shift slightly to higher wave number as the nitrogen content increases (30–40  $\text{cm}^{-1}$  from the undoped to the most heavily doped sample). Such a shift could arise from a slight change in  $sp^2$  domain size,<sup>9</sup> a change in the hydrogen content in the film,<sup>24,25</sup> or the overlap of a  $\text{C}=\text{N}$  band.<sup>15</sup> The fact that no significant change in the  $I(G)/I(D)$  intensity ratio is observed favors the latter possibilities. The ratio and widths of the  $G$  and  $D$  bands for all of the nitrogen-doped samples are consistent with the corresponding Raman data for other diamondlike amorphous carbons.<sup>2,3,9</sup> X-ray diffraction on our samples reveals no sharp lines as expected for an amorphous material. All of the films were quite hard and could not be scratched by sharp stainless-steel tweezers.

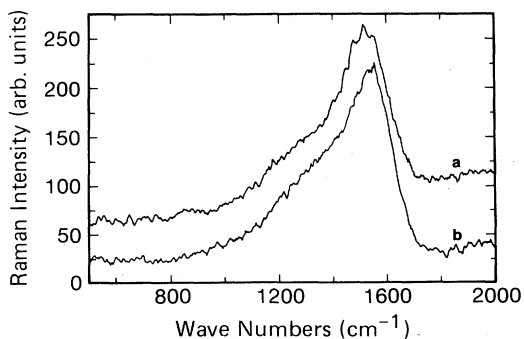


FIG. 2. Raman spectra without (a) and with (b) nitrogen doping. The data were scaled to the  $G$ -band intensities. The relative intensities of the Raman  $G$  and  $D$  bands are approximately the same in all samples.

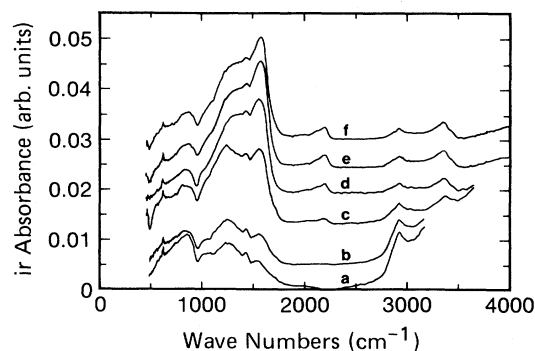


FIG. 3. ir spectra as a function of relative nitrogen concentration. Data were translated but not rescaled (a is undoped, b=2 at. %, c=9 at. %, d=15 at. %, e=18 at. %, f=20 at. % nitrogen).

In Fig. 3 the ir data as a function of the relative nitrogen concentration are shown. No arbitrary scaling factors were introduced, though successive curves are translated upwards for clarity. All spectra exhibit a small background in the 500–2000  $\text{cm}^{-1}$  region. Two strong lines become active in the  $sp^2$  region at approximately 1570 and 1370  $\text{cm}^{-1}$  with increasing nitrogen concentration. A weaker doublet is observed at 2100–2200  $\text{cm}^{-1}$  in the  $sp$  region. CH stretching bands at 2925  $\text{cm}^{-1}$  decrease in intensity with nitrogen doping, and NH stretching modes at 3365  $\text{cm}^{-1}$  appear. Surveys of ir spectra of organic compounds suggest two possible interpretations for the modes in the  $sp^2$  and  $sp$  regions.<sup>26</sup> Carbon-carbon vibrations in aromatic<sup>27</sup> and/or acetylenic<sup>28</sup> groups can become ir active due to the addition of nitrogen at neighboring sites. Alternatively as Han and Feldman suggest,<sup>15</sup> the addition of nitrogen can result in the formation of imino and nitrile groups which are active near 1600 and 2200  $\text{cm}^{-1}$ , respectively. The substitution of  $^{15}\text{N}$  in the plasma was made to determine which modes, if any, arise from carbon-nitrogen vibrations. Figure 4

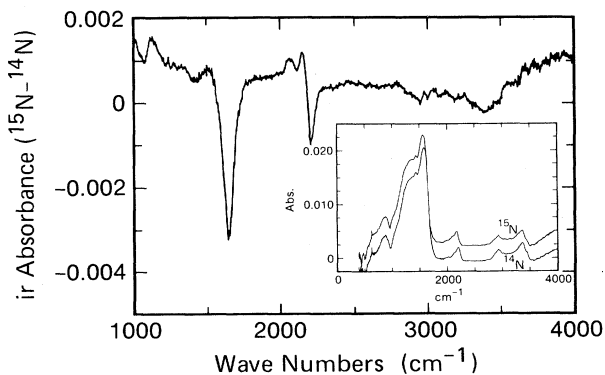


FIG. 4. The ir difference spectrum for 15 at. %  $^{15}\text{N}$ - and  $^{14}\text{N}$ -doped carbon. The derivative shapes at 2100 and 2200  $\text{cm}^{-1}$  are due to isotope shift of the nitrile groups. Absorbance spectra are shown in the inset.

shows the ir difference spectrum for 15 at. %  $^{15}\text{N}$  and  $^{14}\text{N}$ . The absorbance spectra are shown in the inset. The derivative shapes at 2100 and 2200  $\text{cm}^{-1}$  indicate an isotope shift of 31  $\text{cm}^{-1}$  for these lines. The existence of this shift (consistent with literature values) is proof that these modes correspond to carbon-nitrogen triple bonds.<sup>29</sup> We associate the 2200- $\text{cm}^{-1}$  line with a nitrile bound to an aromatic ring. The 2130- $\text{cm}^{-1}$  shoulder could arise from isonitrile, or possibly nitrile in an unusual environment.<sup>26</sup> The observed isotope effect in these samples is an existence proof of  $sp$  carbon in a hard amorphous carbon sample. Robertson states that "there is little evidence for  $sp^1$  sites in unhydrogenated carbons, but there is some evidence for minor amounts of  $-\text{C}\equiv\text{CH}$  groups being present in  $\alpha\text{-C:H}$ ."<sup>30</sup> We have seen the  $sp$  carbon vibration not only in these hard hydrogenated films, but also in nitrogen-doped carbon made by sputtering which shows no evidence of  $\text{CH}_n$  or  $\text{NH}_m$  in the ir.

Also evident in Fig. 4 is a negative peak in the difference spectrum at 1650  $\text{cm}^{-1}$ . Unlike the derivative features observed for the nitrile (which were comparable in intensity to the original peak), the area under the 1650 feature is less than 10% of the  $sp^2$  features. Since control of the doping level is accurate to  $\approx 1\text{--}2$  at. %, and since the intensity of the  $sp^2$  line is sensitive to nitrogen concentration, the 1650 feature is mostly due to a difference in nitrogen concentration. The absence of an isotope shift for the 1370 and 1570 lines proves that these lines are not predominantly nitrogen-containing modes. Since both lines do increase in intensity with nitrogen concentration in the film, they must occur because the presence of the nitrogen causes other vibrations to become ir active. To identify these vibrations, we subtract the contribution of the background intensity in the undoped sample from the ir spectra of the doped samples. Figure 5 shows this difference spectrum for the most heavily doped sample. Also shown in Fig. 5 is the Raman spectrum of the same sample. The close agreement of these data strongly suggests that the nitrogen doping causes the Raman  $G$  and  $D$  bands to become ir active. The shift to higher wave number (with increased nitrogen content) observed for the Raman  $G$  band is also observed in the in-

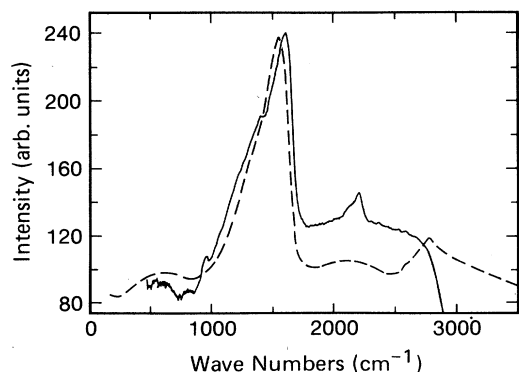


FIG. 5. Comparison of the ir (solid line) and Raman (dashed line) spectra for the most heavily doped samples. The data strongly suggest that nitrogen causes the Raman bands to become ir active.

frared.

These results can be understood if the nitrogen substitutes for a few of the nonbridgehead (i.e., perimeter) carbon atoms in the graphitic microdomains of the films. With nitrogen in the graphite structure, the symmetry of the rings are broken, and the ir forbidden  $E_{2g}$  mode becomes allowed in the plane.<sup>21,22</sup> The comparison of the undoped and doped films is analogous to the case of benzene (six carbon atoms in an aromatic ring), where the 1588  $\text{cm}^{-1}$  mode is forbidden compared to pyridine (five carbons and one nitrogen atom in an aromatic ring), where the corresponding 1590  $\text{cm}^{-1}$  mode is allowed.<sup>26</sup> In our amorphous carbon we can rationalize the intensity increase of the  $G$  band with N substitution if we note that the disruption of the symmetry is maximal when every ring contains at least one nitrogen—about  $\frac{1}{6}$  or 16.7 at. % nitrogen. Of course, this is only possible when the domain sizes are small. If the domain sizes were large, then random N substitution will decrease aromaticity near nitrogen bridgeheads. This would result in a significant change in the Raman  $G$  and  $D$  bands. The fact that the Raman does not change appreciably, and the fact that the  $sp^2$  domain size is small in our samples, indicate that most of the nitrogen dopants break symmetry without affecting aromaticity.

It is well known that hydrogen plays an important role in determining many properties of amorphous carbon films.<sup>7</sup> However, the amount of hydrogen does not seem to alter the effect of the nitrogen on the ir spectra. Nitrogen-doped films made by sputtering of the graphite target alone have ir active  $G$  and  $D$  bands and  $sp$  bands as do the plasma-deposited hydrocarbon films shown in Fig. 3. Furthermore, the lack of CH and NH bands in the ir spectra of the sputtered films indicates an absence of hydrogen-containing groups such as amino or methylene. These observations add further support to our interpretation that nitrogen substitution is responsible for the symmetry breaking of the  $E_{2g}$  mode and the ir intensity of the  $G$  and  $D$  bands.

As discussed above, the relative intensity of the Raman  $G$  and  $D$  bands provides useful information about the structure of amorphous carbons. Unfortunately, Raman spectroscopy is a difficult technique and is not as available as ir. However, the fact that even low levels of nitrogen doping make the Raman information accessible in the infrared, without dramatically changing the  $sp^2$  domain size, suggests that one can use chemical treatments to gain more information about amorphous carbons. In addition to "doing Raman with ir," the good signal-to-noise ratio of the infrared spectra of the most heavily nitrogen-doped films enables us to obtain quantitative estimates of the film composition from the ir data. This is done with the following procedures.

(1) The intensities of the  $G$  band,  $sp$  band,  $\text{CH}_n$  band, and  $\text{NH}_m$  band are measured from the ir spectra.

(2) These intensities are converted to relative concentrations. To accomplish this, we estimate the carbon matrix elements from model compounds (nitrile substituted toluenes).<sup>26</sup> These compounds suggest that the carbon  $sp^3$  intensity is equal to the carbon  $sp^2$  intensity and that

both are approximately half the intensity for the *sp* carbon. To estimate the hydrogen and nitrogen matrix elements we use the fact that the increase in  $NH_m$  is proportional to the increase in *sp* carbon (proportionality factor is 1.34), and the decrease in  $CH_n$  is accompanied by a linear increase in  $NH_m$  (proportionality factor  $-1.15$ ).

(3) From the Raman data, we make the initial assumption that the  $sp^2$  band is constant and due only to carbon  $sp^2$ . This assumption is not exact, and a self-consistency check of the results will provide an upper bound to the relative nitrogen  $sp^2$  concentration.

(4) Normalizing the atomic concentrations for each sample, we obtain estimates, Table II, of the  $sp^3$  carbon,  $sp^2$  carbon, *sp* carbon, nitrogen and hydrogen content as a function of nitrogen doping. For example, from analysis of all the ir data, we predict that the undoped films contains  $\approx 29$  at. % hydrogen,  $\approx 14$  at. % carbon  $sp^3$ , and  $\approx 57$  at. % carbon  $sp^2$ . From this we find  $[sp^2]/[sp^3] \approx 4$ , and an empirical formula for the material of  $C_7H_3$ .

We note that the carbon  $sp^2$  concentration listed in Table II is not constant with respect to nitrogen dopant level. This variation (of about 20%) puts an upper bound on the contribution of nitrogen  $sp^2$  to the *G*-band intensity.

In Fig. 6 we plot the dopant level as  $[N]/([N] + [C]) \equiv ([N]/[C]) / \{[N]/[C] + 1\}$ , where the  $([N]/[C])$  data are taken from Tables I and II. We fit all the compositional data together and the ir data independently to an exponential. In order to compare with the data in Table I, we have renormalized the ir data to exclude hydrogen by plotting the nitrogen content relative to the  $(N+C)$  content in Fig. 6. As discussed above, the symmetry-breaking effect does not seem to depend on hydrogen content as it is also observed in sputtered carbon samples which exhibit no evidence of CH modes in the infrared.

The compositional data ( $[N]/([N] + [C])$ ) saturate at about 17 at. % nitrogen, whereas the ir data saturate somewhat higher at 23%; though the trend is the same. For example, in the most heavily doped film, the ir data suggest 25 at. % hydrogen, 58 at. % carbon, and 17 at. % nitrogen, and therefore the relative nitrogen concentration is  $17/(58+17)$  or 23%. The relative nitrogen concentration as determined by the elemental-analysis techniques, no doubt, provides a better measure than the ir

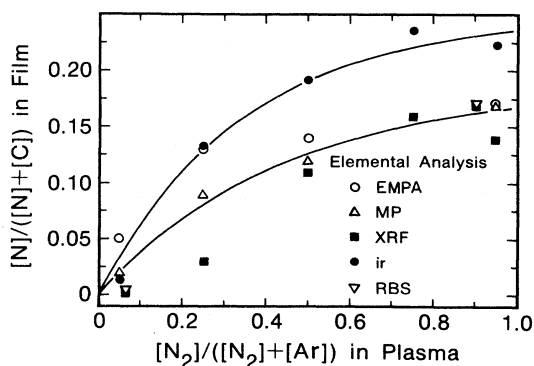


FIG. 6. Elemental analysis (excluding hydrogen) of the nitrogen-doped carbons as a function of nitrogen fraction of the carrier gas in the plasma. The data depict the nitrogen-to-nitrogen+carbon ratio. Hydrogen content is not included but did not vary substantially from film to film. The top curve is a best fit to the infrared data. The lower curve is a best fit to all of the other analytical techniques.

approximation without standards. The intent of the ir analysis was to estimate the hydrogen, carbon *sp*, and carbon  $sp^3$  concentrations which cannot be determined by other techniques. The data in Fig. 6 demonstrates that these estimates are accurate to about 30%. The fact that the nitrogen concentration saturates at one nitrogen per five carbons demonstrates that fairly low dopant levels will break the symmetry of the  $E_{2g}$  mode.

The electronic structure of the doped material does not seem to be strongly affected by the presence of nitrogen. As described above, a bleaching of the fluorescence background is observed with even low levels of nitrogen doping. Conductivity measurements were not possible on samples deposited on conducting substrates, but it was possible to peel off some of the films deposited on gold. The resistivity of the undoped films was too high for measurement on our four-probe equipment. This implies a resistivity over  $10^6 \Omega \text{ cm}$  though we cannot rule out a very large contact resistance.<sup>31</sup> With nitrogen doping, the resistivity of the most highly conducting sample was still over  $100 \Omega \text{ cm}$ . This increase in conductivity could arise from an increase in carrier concentration, or from an increase in carrier lifetime due to elimination of traps.

TABLE II. Estimated  $sp^3$  carbon,  $sp^2$  carbon, *sp* carbon, nitrogen, and hydrogen content as a function of nitrogen doping.

Film	$sp^3$ carbon	$sp^2$ carbon	<i>sp</i> carbon	Total carbon	Total nitrogen	hydrogen
20 at. % $^{14}\text{N}_2$ gas	3	47	9	59	17	24
18 at. %	3	46	9	58	18	24
18 at. % $^{15}\text{N}_2$	3	48	9	60	17	23
15 at. %	4	52	7	63	15	22
9 at. %	7	54	4	65	10	25
2 at. %	13	58	1	72	1	27
0 at. %	14	57		71		29

Evidence for both possibilities is provided by the Raman data which exhibit a decrease in the fluorescence background upon nitrogen doping. Photothermal deflection spectroscopy, on the other hand, provides partial evidence for the former explanation.<sup>32,33</sup> In Fig. 7 we show the PDS spectrum of the band edge for undoped carbon, and carbon doped with about 20% nitrogen. The log-absorbance edge (versus energy) is linear. This exponentially decaying band edge or "Urbach edge" is typical for amorphous materials and is often used as a measure of the degree of disorder. The slope of the edge is roughly equal for the undoped and most heavily doped samples which suggests that the addition of nitrogen does not significantly change the amount of disorder (in good agreement with the Raman results). Without changing slope, the band edge shifts by 0.2 eV to lower energy with doping.<sup>15</sup> Such a shift could result from delocalization of the  $\pi$  electrons, possibly resulting from overlap between neighboring  $sp^2$  microdomains separated by nitrile groups. Alternatively, the shift could result from the creation of defect states near the band edge. More work is required to resolve this issue.

### CONCLUSION

One would expect that the addition of nitrogen to an amorphous carbon film would radically alter the molecular structure of the material. Indeed, the infrared spectrum of carbon changes dramatically upon nitrogen doping. However, the Raman spectrum shows no change in the shape and relative intensities of the  $G$  and  $D$  bands as a function of the level of nitrogen doping. This apparent contradiction is resolved by analyzing the infrared and Raman spectra together. By studying carbons doped with various concentrations of  $^{14}\text{N}$  and  $^{15}\text{N}$ , using both spectroscopic techniques, we have proven that the principal effect of the nitrogen is to distort the molecular symmetry of the  $sp^2$  ring modes. This gives rise to a net dipole moment and the observed ir activity. The intense  $G$  and  $D$  bands are the most dominant feature in the infrared spectrum of the nitrogen-doped carbons. The effect saturates at the maximum nitrogen dopant level of

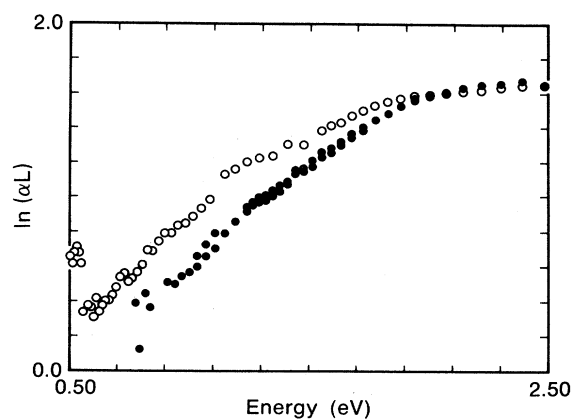


FIG. 7. Photothermal deflection spectrum of undoped (●) and heavily doped carbon (○). The band edge shifts down by  $\approx 0.2$  eV on doping to 17 at. % nitrogen.

about 20% ( $[\text{N}]/[\text{C}] \approx \frac{1}{5}$ ). We note that the nitrogen substitution allows us to measure the Raman  $G$  and  $D$  bands with the infrared spectrometer. Since the infrared measurement records absorbance, it is equally sensitive to all domains within the sample. Furthermore, the ir measurement is also sensitive to  $sp^3$  C—H modes. This makes possible direct comparison of  $sp^2$  and  $sp^3$  concentration with a single measurement. The observation of nitrile, and possibly isonitrile, groups provides the first direct evidence of  $sp$  carbon in amorphous carbon films.

### ACKNOWLEDGMENTS

We wish to thank our many colleagues who made available contributions to this work: Vaughn Deline (RBS), John Duran (SEM), Allen Fung (XRF), Bruce Hoengig and Haj Seki (Raman), Dolores Miller (XPS), Rick Savoy (Microprobe), Andrew Skumanich (PDS), and J. G. Gordon for many useful discussions.

<sup>1</sup>H. Seki, G. M. McClelland, and D. C. Bullock, *Wear* **116**, 379 (1987).

<sup>2</sup>H. Tsai and D. B. Bogy, *J. Vac. Sci. Technol. A* **5**, 3287 (1987).

<sup>3</sup>H. Tsai, D. B. Bogy, M. R. Kundmann, D. K. Veirs, M. R. Hilton, and S. T. Mayer, *J. Vac. Sci. Technol. A* **6**, 2307 (1988).

<sup>4</sup>S. Aisenberg and R. Chabot, *J. Appl. Phys.* **42**, 2953 (1971).

<sup>5</sup>N. Savvides, *J. Appl. Phys.* **58**, 518 (1985).

<sup>6</sup>D. R. McKenzie, R. McPhedran, N. Savvides, and L. C. Botten, *Philos. Mag.* **B 48**, 341 (1983).

<sup>7</sup>J. C. Angus and C. C. Hayman, *Science* **241**, 913 (1988).

<sup>8</sup>K. Enke, *Thin Solid Films* **80**, 227 (1981).

<sup>9</sup>H. Seki, International Conference on Metallurgical Coatings, San Diego, 1988 (in press).

<sup>10</sup>F. Tuinstra and J. L. Koenig, *J. Chem. Phys.* **53**, 1126 (1970).

<sup>11</sup>R. Vidano and D. B. Fischbach, *J. Am. Ceram. Soc.* **61**, 13 (1978).

<sup>12</sup>R. O. Dillon, J. A. Woollam, and V. Katkanant, *Phys. Rev. B* **29**, 3482 (1984).

<sup>13</sup>F. Parmigiani, E. Kay, and H. Seki, *J. Appl. Phys.* **64**, 3031 (1988).

<sup>14</sup>J. Foster and J. Frommer (private communication).

<sup>15</sup>H.-X. Han and B. J. Feldman, *Solid State Commun.* **65**, 921 (1988).

<sup>16</sup>D. J. Jones and A. D. Stewart, *Philos. Mag.* **B 46**, 423 (1982).

<sup>17</sup>N. Voke and J. Kanicki, in *Plasma Processing*, edited by J. W. Coburn, R. A. Gottscho, and D. W. Hess (Materials Research Society, Pittsburgh, 1986), p. 175.

<sup>18</sup>B. N. Khare, C. Sagan, E. Arakawa, F. Suits, T. A. Alcott, and M. W. Williams, *Icarus* **60**, 127 (1984).

- <sup>19</sup>R. A. Friedel and L. J. E. Hofer, *J. Phys. Chem.* **74**, 2921 (1970).
- <sup>20</sup>R. G. Greenler, *J. Chem. Phys.* **44**, 310 (1966).
- <sup>21</sup>S. A. Solin, *Physica* **99B**, 443 (1980).
- <sup>22</sup>M. P. Conrad and H. L. Strauss, *Phys. Rev. B* **31**, 6669 (1985).
- <sup>23</sup>M. Yoshikawa, G. Katagiri, H. Ishida, H. Ishitani, and T. Akamatsu, *Appl. Phys. Lett.* **52**, 1639 (1988).
- <sup>24</sup>D. Beeman, J. Silverman, R. Lynds, and M. R. Anderson, *Phys. Rev. B* **30**, 870 (1984).
- <sup>25</sup>A. Richter, H.-J. Scheibe, W. Pompe, K.-W. Brzezinka, and I. Muhling, *J. Non-Cryst. Solids* **88**, 131 (1986).
- <sup>26</sup>See, e.g., N. B. Colthup, L. H. Daly, and S. E. Wiberley, *Introduction to Infrared and Raman Spectroscopy*, 2nd ed. (Academic, New York, 1975).
- <sup>27</sup>R. A. Friedel and G. L. Carlsen, *Fuel* **51**, 194 (1972).
- <sup>28</sup>See, e.g., C. Wentrup, *et al.*, *J. Am. Chem. Soc.* **110**, 1337 (1988).
- <sup>29</sup>S. Pinchas and I. Laulicht, *Infrared Spectra of Labelled Compounds* (Academic, New York, 1971), p. 216.
- <sup>30</sup>J. Robertson, *Adv. Phys.* **25**, 317 (1987).
- <sup>31</sup>The four-point probe is, of course, designed to be insensitive to contact resistance. However, if the contact resistance is sufficiently high, the outer probes will not supply sufficient current for an accurate voltage reading. This can occur even if the intrinsic resistivity is less than  $10^6 \Omega \text{ cm}$ .
- <sup>32</sup>W. B. Jackson, N. M. Amer, A. C. Boccara, and D. Fournier, *Appl. Opt.* **20**, 1333 (1981).
- <sup>33</sup>N. M. Amer and W. B. Jackson, in *Semiconductors and Semimetals*, edited by J. I. Pankove (Academic, New York, 1984), Vol. 21, Part B, p. 83.